

# Poling and its relaxation studies of polycarbonate and poly(styrene-*co*-acrylonitrile) doped by a nonlinear optical chromophore

Abdelkarim Mohamed Abo El Wafa<sup>a,b,\*</sup>, Shuji Okada<sup>b</sup>, Hachiro Nakanishi<sup>b</sup>

<sup>a</sup> Polymer Laboratory, Physics Department, Faculty of Science, Mansoura University, Mansoura 35516, Egypt

<sup>b</sup> Institute of Multidisciplinary Research for Advanced Materials (IMRAM), Tohoku University, Sendai 980-8577, Japan

Received 10 October 2004; received in revised form 12 November 2004; accepted 22 March 2005

Available online 9 June 2005

## Abstract

Spin-coated films of poly(bisphenol A carbonate) (PC) and poly(styrene-*co*-acrylonitrile) (SAN) doped by 4-(*N,N*-dimethylamino)-4'-nitrostilbene (DANS) were prepared, and their poling and depoling behaviors were investigated mainly by UV–visible absorption spectra and second-harmonic generation (SHG). The absorbance of DANS in the PC and SAN films proportionally increased with increasing its weight concentration up to 5 wt%, indicating homogeneous dissolution of DANS in the host polymers. However, above this concentration, heterogeneous structures due to DANS crystallites could be observed under a polarizing microscope. Poling of the films was performed using a triode corona discharging system. The maximum *d* coefficients were obtained at slightly lower poling temperature than the glass transition temperature of the corresponding dye-doped polymer. The KWW stretched exponential function could be fitted to the experimental temporal relaxation data of SHG for the SAN system. Relatively high long-term stability was observed for the PC system because of its relatively rigid backbone structure.  
© 2005 Elsevier Ltd. All rights reserved.

**Keywords:** PC; SAN; DANS; SHG; Dipole relaxation; Backbond and heterogeneous structure; Glass transition and temporal stability

## 1. Introduction

The development of thin film polymer materials suitable for the fabrication of high-speed integrated optical devices is presently a major focus of research on nonlinear optical (NLO) materials [1–4]. Polymer materials with proper alignment of NLO chromophores have been demonstrated to possess large NLO properties compared with traditional inorganic materials. Low intrinsic dielectric constant; easy processing into thin

films and compatibility with microelectronic processes are the other major advantages of polymers. Significant progress in device design and architecture with implementation of poled polymers into prototype electro-optical devices has been reported recently [5,6]. Since the orientational distribution of NLO chromophores in the unpoled polymer films is isotropic, the corona-triode poling at elevated temperature is often used for producing NLO polymer films [7]. The NLO effects of poled polymers originate from large hyperpolarizability of the chromophores and their noncentrosymmetric alignment by the applied electric field.

In this paper, we report the poling and successive relaxation behaviors of dye-doped polymer systems. The polymer investigated were the polycarbonate (PC) and

\* Corresponding author. Present address: Research Institute of Electronics, Shizuoka University, 3-5-1 Johoku Hamamatsu 432-8011, Japan. Fax: +81 53 478 1312.

E-mail address: [karimegjp@hotmail.com](mailto:karimegjp@hotmail.com) (A.M.A. El Wafa).

poly(styrene-co-acrylonitrile) (SAN). Although PC-based dye-doped NLO polymers have been reported [8,9], SAN has not been used as a polymer matrix for second-order NLO materials to our knowledge. As a doping dye, 4-(*N,N*-dimethylamino)-4'-nitrostilbene (DANS) was selected because it has larger molecular size than *p*-nitroaniline derivatives [10] and higher melting point at 523 K compared with the conventional azo-dyes. The NLO coefficients for second-harmonic generation (SHG) were evaluated by the Maker-fringe method and the temporal stability of the poled polymer was monitored by SHG intensity. The factors influencing the SHG intensity and its relaxation, such as the poling temperature, applied electric field and poling time were studied.

## 2. Experimental

### 2.1. Materials

PC used was poly(bisphenol A carbonate) ( $M_w = 28,800$ ) obtained from Aldrich Chemical Co., Inc. SAN (styrene:acrylonitrile = 75:25) was obtained from Polysciences Inc. DANS was purchased from Fluka. These polymers and the organic dye were used as received.

### 2.2. Film preparation

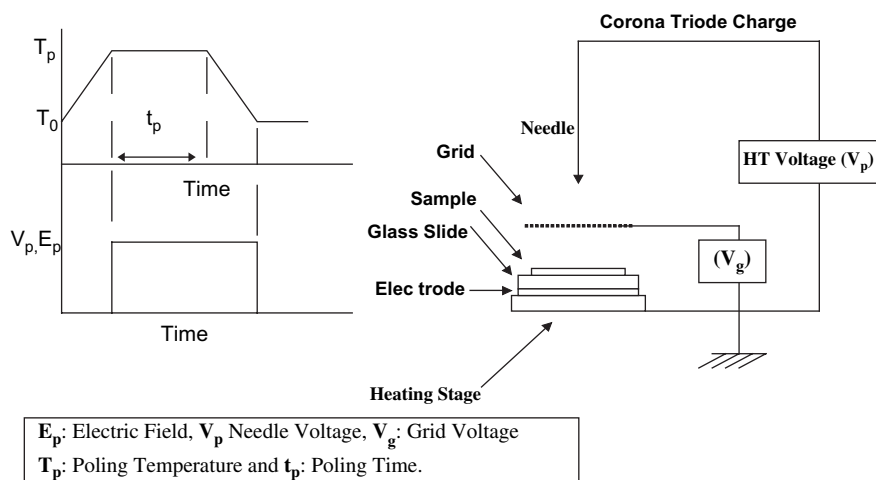
For UV–visible analysis and SHG measurements, films were prepared by the spin-coating method. The mixed solution of a polymer and the dye was spin-coated at room temperature with the spinning rate of 1000 rpm on to glass. Spin-coated films were dried at room temperature for one day. The film thicknesses thus prepared were 0.5–1  $\mu\text{m}$ . The film samples for DSC were prepared by the casting method in aluminum pans and dried at 323 K for two days.

### 2.3. Corona poling process

Scheme 1 illustrates the circuit used for corona discharging. The corona voltage was kept at a certain value in the range of 6–11 kV and the grid voltage was varied in the range from 0 to 1 kV to obtain the desired poling field  $V_g/L$ , where  $V_g$  is the grid voltage and  $L$  is the film thickness [11]. The grid was kept about 4 mm from the film surface. The discharging process was continued for a certain time  $t_p$  at a desired temperature  $T_p$  and applied voltage was still on even during subsequent cooling process to room temperature.

### 2.4. Characterization techniques

UV–visible spectra were obtained using a Jasco V-570 spectrometer. Differential scanning calorimetry (DSC) scans were carried out using a Perkin Elmer Pyris Diamond DSC apparatus over the temperature range from 293 K to 473 K with heating rate of 20 K/min. The SHG of the dye-doped polymer films was measured by the Maker-fringe method [12–14] using a Q-switched Nd:YAG laser at 1064 nm (Coherent Infinity 40–100). Pulse width was about 3.5 ns, and pulse energy was reduced to ca. 10 mJ. The second-order NLO coefficients ( $d_{33}$ ) of the polymer films were obtained using a Y-cut quartz crystal plate ( $d_{11} = 0.5 \text{ pm V}^{-1}$ ) with 1 mm thickness as a reference. Measurements of film thickness were performed using a Dektak<sup>3</sup>ST surface profiler. Refractive indices were measured with a Metricon prism coupler (model 2010). The SHG signal intensity of the poled samples was also measured while the samples were isothermally heated at a fixed temperature in the range of 333–393 K. In this measurement, the incident angle of the fundamental beam was set at 45°, and temporal SHG intensity change was monitored.



Scheme 1. Schematic diagram of the applied field  $E_p$  or voltage  $V_p$ , temperature  $T_p$  and holding time  $t_p$  in the poling process (left), and experimental set-up of corona-triode discharge (right).

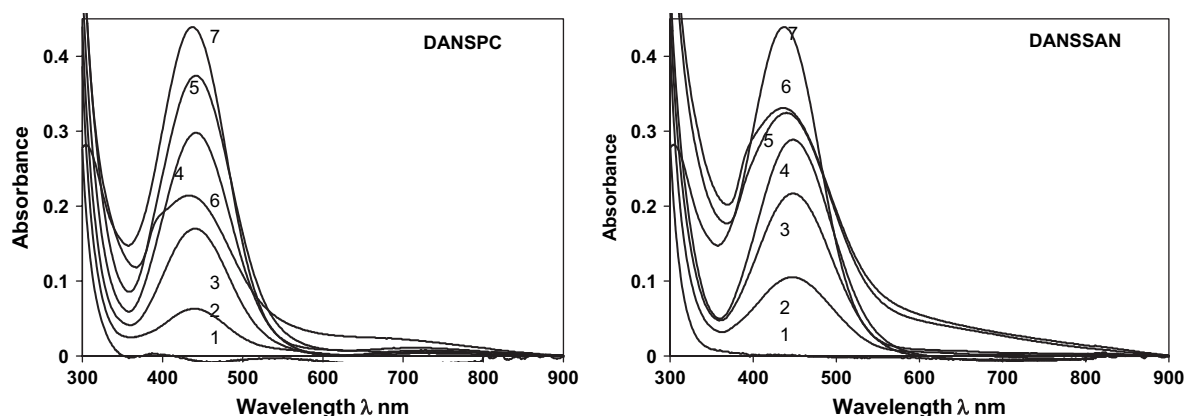


Fig. 1. Absorption spectra of pure and DANS-doped PC (a) and SAN (b). The curve 7 indicates the spectra of DANS chloroform solution. Other numbers in the figure indicate the samples with different DANS weight contents as follows: 1, 0 wt%; 2, 1 wt%; 3, 3 wt%; 4, 5 wt%; 5, 7.5 wt%; 6, 10 wt%.

### 3. Results and discussion

The UV–visible absorption spectra for the two investigated polymers, i.e. DANS-doped PC and SAN, with different concentrations are shown in Fig. 1. Up to 5 wt% concentration of DANS, the absorbance at the absorption maximum proportionally increases with increasing dye concentration. However, when the concentration increased more than 5 wt%, increasing rate of the absorbance dropped. In addition, the shape of absorption bands was deformed and absorption tail was extended to about 900 nm due to light scattering. These observations indicate that DANS molecules start to aggregate to form crystallites in the polymer when the weight concentration is more than 5 wt% [15]. The crystallization states of DANS were observed for 10 wt% DANS-doped SAN using a polarizing optical microscope as shown in Fig. 2. As was expected from the spectroscopic results, DANS crystallites were observed as bright dots (Fig. 2(a)). In order to dissolve

these crystallites in the polymer matrix, the sample was heated. Number of the crystallites decreased by heating and completely disappeared at 473 K to give a homogeneous film (Fig. 2(b)). This homogeneous state maintained longer than several months. UV–visible spectral change between before and after heating for the same sample is shown in Fig. 3. It is clear that the absorbance of the band increases and the absorption tail shifts to the shorter wavelength; this result can be explained by dissolution of the dye crystallites into polymer matrix.

Poling parameters such as poling voltage ( $V_p$ ), grid voltage ( $V_g$ ), poling time ( $t_p$ ) and poling temperature ( $T_p$ ) were varied to find appropriate conditions for the present polymer systems doped by 5 wt% DANS. Poling efficiency was evaluated by  $d_{33}$  values of the samples.  $V_p$  was changed from 7 kV to 11 kV since  $V_p$  more than 11 kV resulted in break-down damages to the samples, and maximum efficiency was obtained at 11 kV.  $V_g$  of 0.5 kV and  $t_p$  of 15 min were found to be the most efficient conditions among the tested parameters.

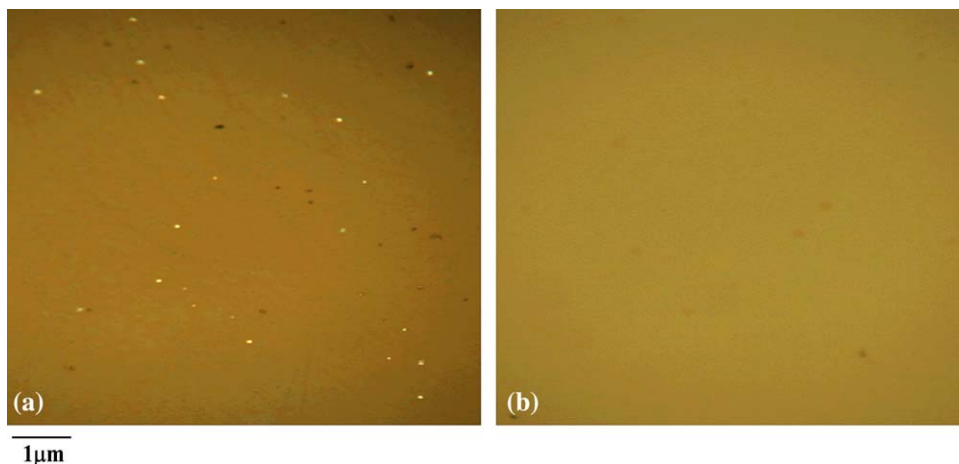


Fig. 2. Morphology of the 10 wt% DANS-doped SAN film: (a) as prepared film and (b) after heating at 473 K for 5 min.

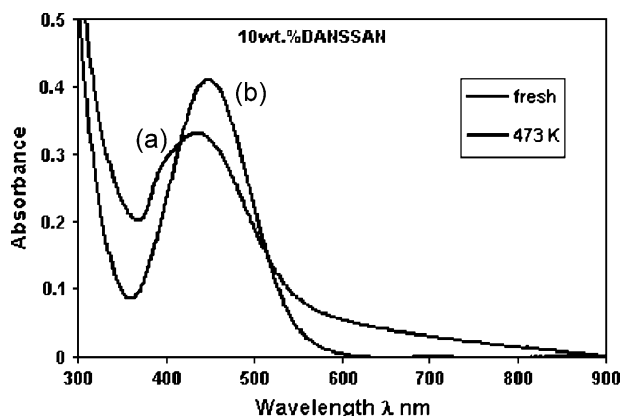


Fig. 3. UV–visible spectra of the 10 wt% DANS-doped SAN film: (a) as prepared film and (b) after heating at 473 K for 5 min.

The largest  $d$  values were obtained when  $T_p$  was set at 373 K for PC and 363 K for SAN. These values were compared with the glass transition temperatures ( $T_g$ s) of the polymer systems. As shown in Fig. 4, pure PC and SAN have  $T_g$ s at 423 K and 381 K, respectively, and  $T_g$  decreased monotonically by increasing the doped dye content. For 5 wt% DANS, doped PC and SAN systems showed  $T_g$ s at 386 K and 366 K, respectively, which were slightly higher than the most efficient  $T_p$ s. The maximum  $d_{33}$  values obtained for DANS-doped PC and SAN were  $1.2 \text{ pm V}^{-1}$  and  $1.6 \text{ pm V}^{-1}$ , respectively. Reason why SAN system showed larger  $d$  value may be due to larger local mobility and free volume of SAN compared with PC possessing a sufficiently rigid backbone [16]. Although homogeneous films of 10 wt% DANS-doped SAN were obtained by post-heating treatment, the  $d_{33}$  values obtained were smaller than those of 5 wt% doped SAN.

Analysis of relaxation process of 5 wt% DANS-doped PC and SAN after poling at optimum condition was examined using spectroscopic methods. The UV–visible spectra of 5 wt% DANS-doped PC films stored

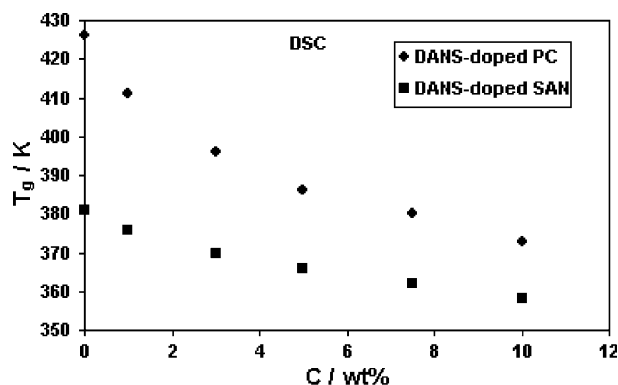


Fig. 4. Glass transition temperature ( $T_g$ ) change depending on DANS weight concentration ( $c$ ) in PC or SAN.

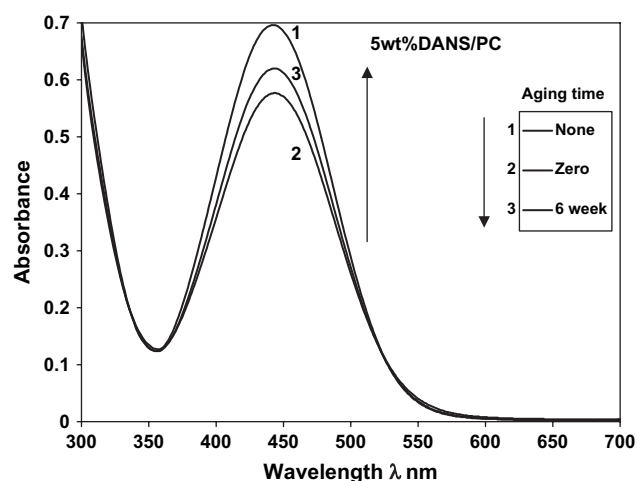


Fig. 5. UV–visible spectra of the 5 wt% DANS-doped PC film before corona poling, after poling at 373 K for 15 min ( $V_p = 11 \text{ kV}$  and  $V_g = 0.5 \text{ kV}$ ) and after keeping in air at room temperature for six weeks after poling.

at room temperature display an increase of the absorption maximum band with time (Fig. 5), indicating relaxation of the dye orientation. At room temperature in air,  $d_{33}$  values of 5 wt% DANS-doped PC and SAN remained about 67 and 78%, respectively, of its initial values after 42 days.

The SHG intensity change during isothermal heating was measured in the range of 333–393 K for 5 wt% DANS-doped SAN. Fig. 6 shows the time dependence of  $I/I_0$ , where  $I$  is the SHG signal intensity at time  $t$  and  $I_0$  is its initial value. The SHG signal decay due to large dopant mobility and local free volume in the glassy matrix [17] was observed more rapidly at higher temperature. The orientation relaxation phenomena of the NLO activity can be empirically described by the Kohlrausch–Williams–Watts (KWW) stretched exponential function [18] as follows:

$$y = \frac{I}{I_0} = \exp \left[ - \left( \frac{t}{\tau} \right)^\beta \right], \quad (1)$$

where  $y$  represents the normalized SHG intensity,  $\tau$  is a characteristic relaxation time and  $\beta$  is a parameter with values between 0 and 1. The  $\beta$  value reflects the distribution breadth of relaxation times or measures the cooperative relaxation processes. Eq. (1) can be transformed as

$$\ln(y) = - \left( \frac{t}{\tau} \right)^\beta \quad (2)$$

or

$$\ln|\ln(y)| = \beta \ln(t) - \beta \ln(\tau). \quad (3)$$

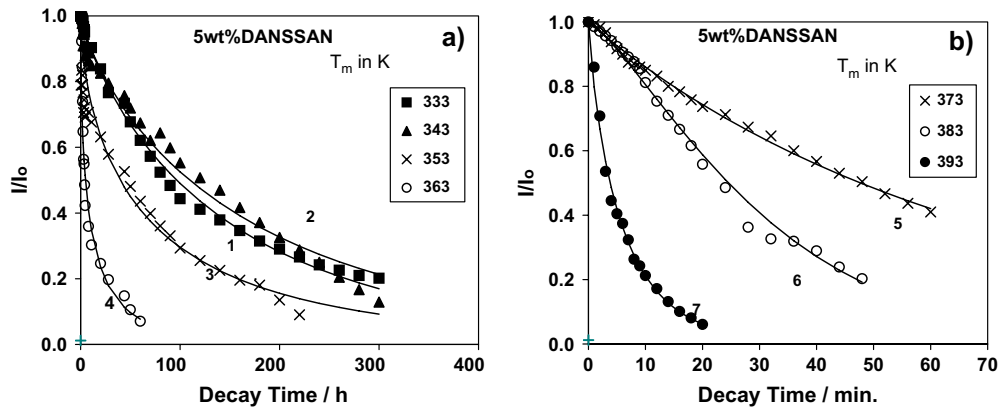


Fig. 6. Decay of normalized SHG intensity due to dye-orientation relaxation process at various temperatures for the 5 wt% DANS-doped SAN poled at 363 K for 15 min with  $V_p = 11$  kV and  $V_g = 0.5$  kV. The solid lines are fitted curves obtained by KWW stretched exponential function.

We plotted  $\ln|\ln(y)|$  against  $\ln(t)$  from the results in Fig. 6 as shown in Fig. 7. From the intercept and the slope of the fitting line, we could obtain the  $\tau$  and  $\beta$  values as displayed in Fig. 8. The significant decrease in  $\tau$  started at around 350 K, and exponential decrease in  $\tau$  continued up to 393 K through  $T_g$  at 366 K. On the other hand,  $T_g$  is more critical for  $\beta$ . Below  $T_g$ ,  $\beta$  decreased from 0.88 to 0.52 with increasing temperature up to 363 K. However,  $\beta$  value jumped to near 1 above  $T_g$ . Large  $\beta$  values are known to reflect the less breadth in the distribution of relaxation times or the reduction in the number of chain segments, which participate in a particular relaxation. Below  $T_g$ , the number of chain segments for the relaxation process should increase with increasing temperature, resulting in decrease of  $\beta$  with increasing temperature. Since almost all side chains

are freely mobile above  $T_g$ , the relaxation time distribution may be near 1.

The similar experiments were also carried out for DANS-doped PC systems. However, their relaxation behavior was more complicated than those of SAN systems, and the KWW exponential function could be applied at only limited temperatures. At these temperatures,  $\tau$  was always longer than that of the corresponding SAN system at the same temperature. The higher temporal stability in the DANS-doped PC may be due to thermal detrapping of charge carriers and rigid backbone structure of PC [16].

#### 4. Conclusion

We have prepared PC and SAN films doped by DANS with weight concentration up to 10 wt%, and found that 5 wt% of DANS was the maximum concentration for the uniform structure without crystallites, confirmed by UV–visible spectra and morphology observation by the optical microscope. The corona-triode poling was performed for these films in a variety of conditions and the most effective poling temperature was found to be slightly lower than  $T_g$  of the corresponding doped polymer. The maximum  $d_{33}$  values obtained for DANS-doped PC and SAN were  $1.2 \text{ pm V}^{-1}$  and  $1.6 \text{ pm V}^{-1}$ , respectively. For SAN system, depoling process was investigated by isothermal heating. The relaxation behaviors could be fitted by using KWW function. Although the relaxation time  $\tau$  was not so related to  $T_g$ , relaxation parameter  $\beta$ , which related to distribution breadth of relaxation times or the cooperative relaxation processes, was found to be critical for  $T_g$ . For PC system, the temporal stability was found to be higher than that of SAN system although relaxation process was more complicated.

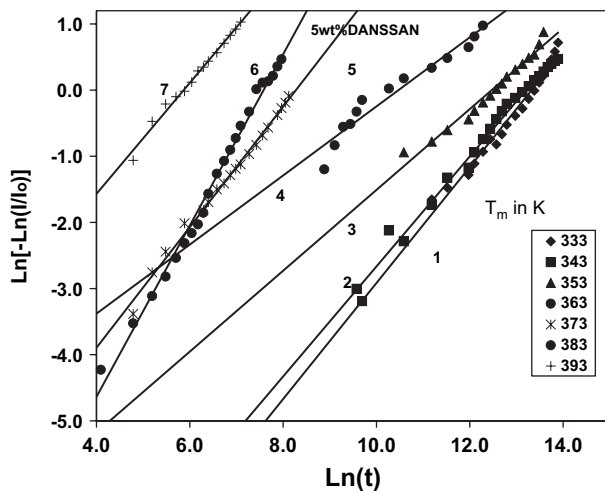


Fig. 7.  $\ln[-\ln(I(t)/I(0))]$  plotted against  $\ln(t)$  at different heating temperature for the poled films of 5 wt% DANS-doped SAN.

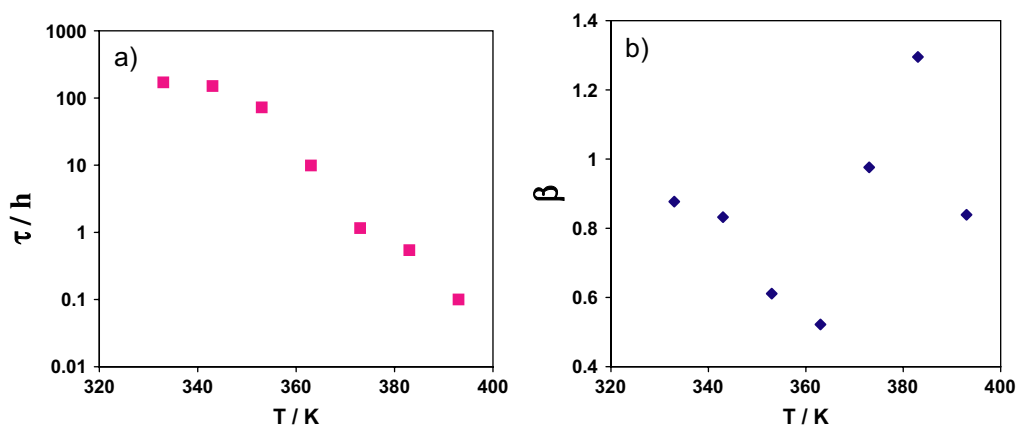


Fig. 8. Relationship between temperature ( $T$ ) and parameters of KWW stretched exponential function, i.e.  $\tau$  (a) and  $\beta$  (b), for the poled films of 5 wt% DANS-doped SAN.

## References

- [1] Burland DM, Miler RD, Walsh CA. *Chem Rev* 1994;94:31.
- [2] Marder SM, Kippelen B, Jen AKY, Peyghambarian N. *Nature* 1997;388:845.
- [3] Marder SR, Perry JW. *Science* 1997;263:1706.
- [4] Jiang H, Kakkar AK. *Adv Mater* 1998;10:1093.
- [5] Dalton LR. *Chem Ind* 1997;7:510.
- [6] Chen A, Chuyanov V, Garner S. *Opt Lett* 1998;23:4787.
- [7] Mortazavi MA, Knoesen A, Kowel ST. *J Opt Soc Am B* 1989;6:733.
- [8] Karakus Y, Bloor D, Cross GH. *J Phys D Appl Phys* 1992;25:1014.
- [9] Wan F, Carlisle GO, Koch K, Martinez DR. *J Mater Sci Mater Electron* 1995;6:228.
- [10] Hampsh HL, Yang J, Wong GK, Torkelson JM. *Polym Commun* 1989;30:40.
- [11] Hundal JS, Nath R. *J Phys D Appl Phys* 1998;31:482.
- [12] Maker PD, Terhune RW, Nisenoff M, Savage CM. *Phys Rev Lett* 1962;8:21.
- [13] Jerphagnon J, Kurtz SK. *J Appl Phys* 1970;40:1667.
- [14] Prasad PN, Williams DJ. In: Prasad PN, Williams DJ, editors. *Introduction to nonlinear optical effects in molecules and polymers*. New York: Wiley-Interscience; 1991 [chapter 6].
- [15] Kimura T, Duan XM, Kato M, Okada S, Yamada S, Matsuda H, et al. *Polymer* 1998;39:491.
- [16] Healy D, Bloor D, Gray D, Cross GH. *J Appl Phys* 1997;30:3079.
- [17] Hampsch HL, Yang J, Wong GK, Torkelson JM. *Macromolecules* 1990;23:3640.
- [18] Singer K, King L. *J Appl Phys* 1991;70:127.